รายงานวิจัยฉบับสมบูรณ์

พฤติกรรมระยะยาวของท่อฝังในคูที่ถมกลับด้วยทรายและก่อสร้างอยู่ในดินเหนียวสำหรับสภาพดินในประเทศไทย

Long-term behavior of pipe embedded in sand trench constructed in clay for soil condition in Thailand

สยาม ยิ้มศิริ

โครงการวิจัยประเภทงบประมาณเงินรายได้จากเงินอุดหนุนรัฐบาล
(งบประมาณแผ่นดิน) ประจำปีงบประมาณ พ.ศ. 2560
มหาวิทยาลัยบูรพา

รหัสโครงการ 2560A10802132

สัญญาเลขที่ 108/2560

รายงานวิจัยฉบับสมบูรณ์

พฤติกรรมระยะยาวของท่อฝังในคูที่ถมกลับด้วยทรายและก่อสร้างอยู่ในดินเหนียวสำหรับสภาพดินในประเทศไทย

Long-term behavior of pipe embedded in sand trench constructed in clay for soil condition in Thailand

สยาม ยิ้มศิริ

คณะวิศวกรรมศาสตร์ มหาวิทยาลัยบูรพา

กรกฎาคม 2561

กิตติกรรมประกาศ

งานวิจัยนี้ได้รับทุนสนับสนุนการวิจัยจากงบประมาณเงินรายได้จากเงินอุดหนุนรัฐบาล (งบประมาณแผ่นดิน) ประจำปีงบประมาณ พ.ศ. 2560 มหาวิทยาลัยบูรพา ผ่านสำนักงานคณะกรรมการการวิจัยแห่งชาติ เลขที่สัญญา 108/2560

บทคัดย่อ

งานวิจัยนี้ทำการศึกษาพฤติกรรมของท่อที่ถูกถมกลับในคูทรายในพื้นที่ดินเหนียวซึ่งเป็นสภาพสำหรับท่อเพื่อการชลประทาน การศึกษาดำเนินการโดยการวิเคราะห์ไฟไนต์เอลิเมนต์เพื่อประเมิน (i) ผลกระทบของขนาดของคู, (ii) ผลกระทบของการจำลองผิวสัมผัสระหว่างทรายถมและดินเดิม และ (iii) ผลกระทบของการจำลองขั้นตอนการก่อสร้าง ผลการศึกษานี้ทำให้สามารถเข้าใจพฤติกรรมของท่อในสภาวะดังกล่าวและทราบเทคนิคการวิเคราะห์ปัญหาโดยวิธีไฟไนต์เอลิเมนต์

ABSTRACT

Finite element analysis is performed in this study to investigate the pipeline-soil interaction of a pipe buried in sand trench embedded in soft clay. This situation is often encountered for pipes used for irrigation purpose. The effects of trench dimensions, the effects of modelling interface between sand backfill and clay trench, and the effects of modelling construction sequences on the pipeline-soil interaction are investigated. The investigation also includes assessment of suitable numerical simulation techniques and procedures for this kind of problem.

สารบัญ

หน้า

กิตติกรรมประกาศ i

บทคัดย่อ ii

สารบัญ iii

Chapter 1 Introduction

Chapter 2 Underground pipe for irrigation purpose

2.1 Recommendation for standard practice by ASTM 2-1

2.2 Investigating parameters 2-2

2.2.1 Effects of trench dimensions 2-2

2.2.2 Effects of modelling interface between sand and clay 2-3

2.2.3 Effects of modelling construction sequences 2-4

Chapter 3 Finite element analysis

3.1 General 3-1

3.2 Soil models 3-3

3.2.1 Mohr-Coulomb soil model 3-3

3.2.2 Clay plasticity soil model 3-5

3.3 Input parameters 3-8

3.3.1 Pipe 3-8

3.3.2 Sand backfill 3-8

3.3.3 Clay 3-9

3.3.4 Interface between pipe and sand 3-9

3.3.5 Interface between sand and clay 3-9

3.4 Finite element analysis procedures 3-10

3.4.1 Without construction sequences modelling 3-10

3.4.2 With construction sequences modelling 3-11

3.4.3 Dummy elements 3-12

3.5 Finite element analysis program 3-12

Chapter 4 Finite element analysis results

4.1 Effects of trench width and depth 4-3

4.2 Effects of modelling interface between sand and clay 4-7

4.3 Effects of modelling construction sequences 4-12

Chapter 5 Conclusions

เอกสารอ้างอิง R-1

Chapter 1 Introduction

Finite element analysis is performed in this study to investigate the long-term pipeline-soil interaction of a pipe buried in sand trench embedded in soft clay. This situation is often encountered for pipes used for irrigation purpose. The ultimate aim is to propose a better pipeline design method for the long-term condition. The effects of trench dimensions, the effects of modelling interface between sand backfill and clay trench, and the effects of modelling construction sequences on the pipeline-soil interaction are investigated. The investigation also includes assessment of suitable numerical simulation techniques and procedures for this kind of problem.

Chapter 2 Underground pipe for irrigation purpose

2.1 Recommendation for standard practice by ASTM

ASTM gives recommendations on the construction of underground pipe for irrigation purpose in its ASTM designation: F 690-86 "Standard Practice for Underground Installation of Thermoplastic Pressure Piping Irrigation Systems". A typical trench cross-section is shown in Fig. 2-1 with important terminologies. The recommendations can be summarised as follows.

- Trench width: Trench width should allow sufficient and safe working room for proper alignment and assembly of the joints. Generally, a trench width at the top of the pipe of about 2 ft (600 mm) wider than the pipe diameter is adequate. However, for pipe with an 18-in. (457-mm) diameter and larger in a vertical-walled trench, a clearance of 3 ft (1 m) wider than the nominal pipe size may be needed.
- Bedding: A depth of from 100 to 150 mm (4 to 6 in.) is generally sufficient to provide bedding.
- Minimum earth cover: Protection from traffic loading should be considered when establishing minimum earth cover requirements. For installations exposed to normal farm vehicle traffic, the minimum total cover should not be less than:-

Pipe 1 to 2½ in. in diameter:	18 in. (450 mm)
Pipe 3 to 4 in. in diameter:	24 in. (600 mm)
Pipe 5 to 18 in. in diameter:	30 in. (750 mm)
Pipe 18 in. and larger in diameter:	36 in. (900 mm)

- Bedding material: The bedding material should consist of gravel, sand, silty sand, silty gravel, or clayey sand in granular form and having a maximum size of 3/4 in. (19 mm).
- Backfill material: The most recommended backfill material is coarse-grained soil containing less than 5% fines, such as clean (that is, essentially silt free), gravels or sands (the maximum density will be obtained by saturation and vibration).

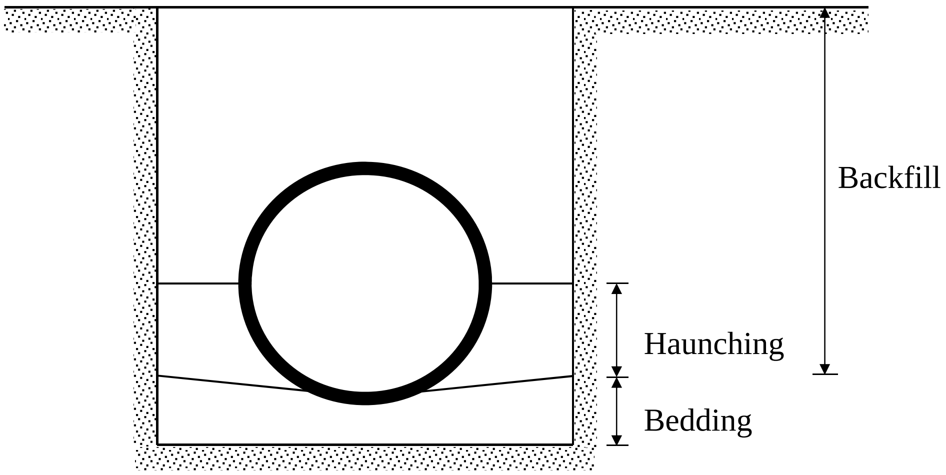

Figure 2-1 Trench cross-section showing terminology

2.2 Investigating parameters

2.2.1 Trench dimensions

The effects of trench dimensions on the pipeline-soil interaction are investigated by performing the finite element analysis at different trench depths (2.0 and 3.0 m to the base of the pipe) and widths (1.5 and 2.0 m). The dimensions of these four cases are shown in Fig. 2-2. The proposed trench dimensions are based on the ASTM recommendations given in Section 2.1.

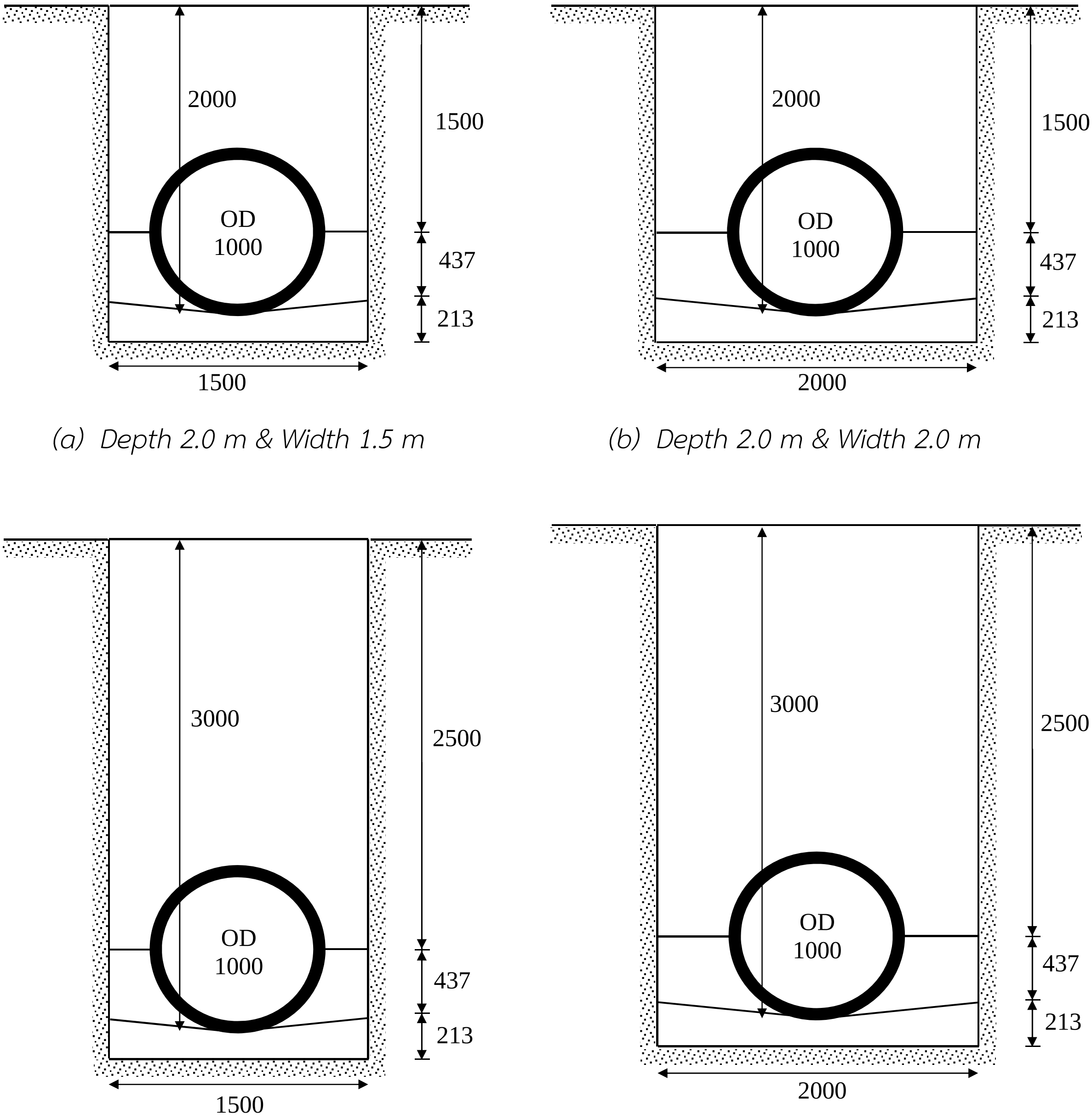

(a) Depth 2.0 m & Width 1.5 m *(b) Depth 2.0 m & Width 2.0 m*

(c) Depth 3.0 m & Width 1.5 m *(d) Depth 3.0 m & Width 2.0 m*

unit in mm

Figure 2-2 Trench dimensions for FE analysis

2.2.2 Interface between sand and clay

The importance of modelling the interface between sand backfill and clay trench is investigated by comparing the FE analysis results from the cases of with and without sand/clay interface. The presence of the interface allows sand and clay to slip relative to each other. The interface between pipe and sand is always modelled in all FE analysis.

2.2.3 Construction sequences

The importance of modelling the construction sequences is investigated by comparing the FE analysis results from the cases of with and without construction sequences modelling. For the case of without construction sequences modelling, the sand (bedding, haunching, and backfill) and pipe are placed into the trench simultaneously within a very short time. For the case of with construction sequences modelling, the backfilling of the trench is done in step-by-step by placing bedding and pipe, haunching, and backfill, in order.

Chapter 3 Finite element analysis

3.1 General

The FE analysis was carried out using ABAQUS. The geometry and constituent elements of the FE model are summarise in Fig. 3-1. The analysis was performed in plane strain condition. The side and bottom boundaries were assumed to be smooth and supported only in the normal direction. The symmetry of the problem was taken into account and only one-half of the problem was analysed. The sand and pipe were represented by 8-node biquadratic displacement, reduced integration continuum elements, whereas the clay was represented by 8-node biquadratic displacement, bilinear pore pressure, reduced integration continuum elements. The sand behaviour was modelled using Mohr-Coulomb model, whereas the clay behaviour was modelled using clay plasticity model. The pipe was assumed as a linear elastic material (ASTM F 679-86: type T-2). The interaction between the pipe and surrounding sand was modelled by surface-based contact simulation by which the slip and separation between the pipe and sand is allowed. An example of the finite element mesh used for the analysis is shown in Fig. 3-2. The element numbers range from 1900 (2-m trench depth) to 2200 (3-m trench depth), which are found to be acceptable after examining the effect of mesh size.

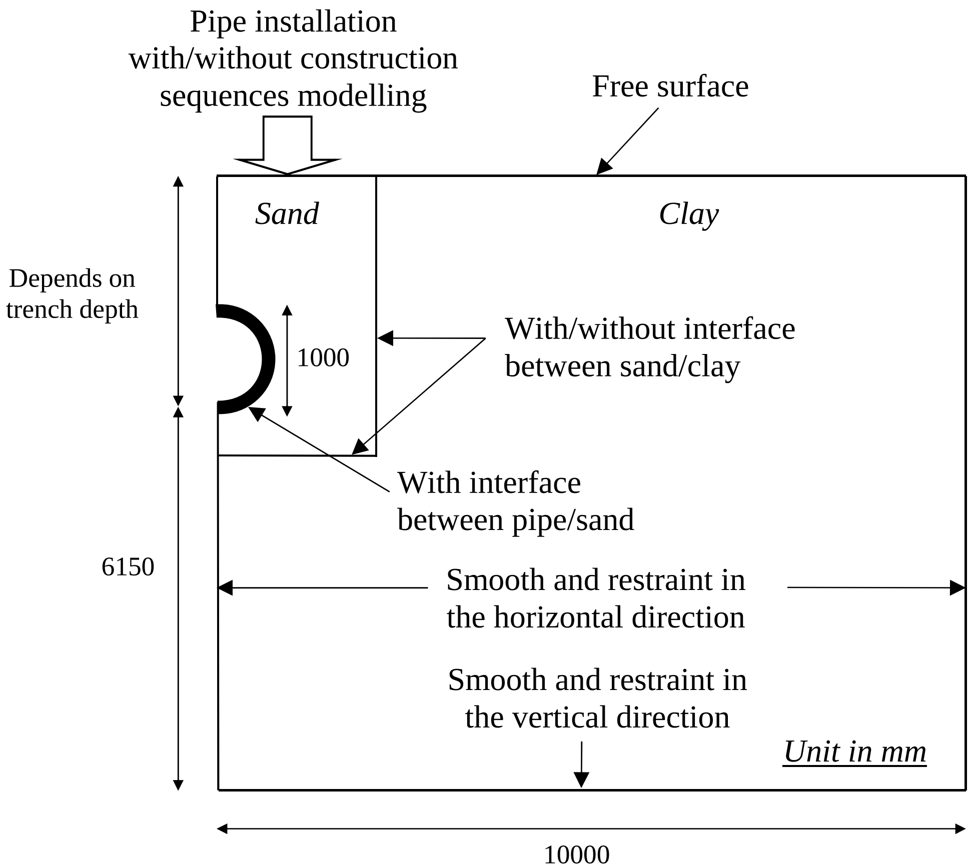

Figure 3-1 FE model geometry and constituent elements

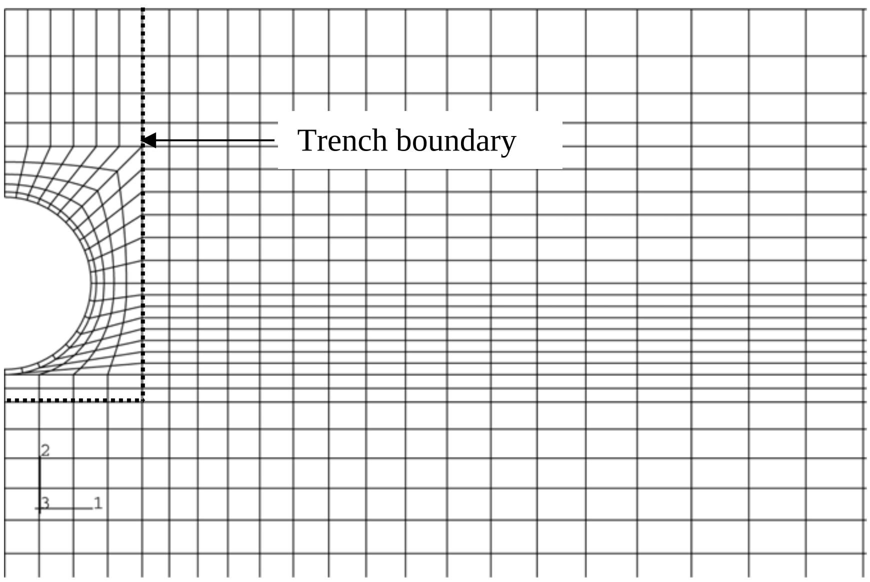

Figure 3-2 Example of FE mesh (depth 2.0 m and width 1.5 m trench)

3.2 Soil models

3.2.1 Mohr-Coulomb soil model

Mohr-Coulomb model is a linear elastic-perfectly plastic model. The users need to specify Young's modulus *E* and Poisson's ratio ν for its elastic behaviour and friction angle ϕ_{max}, dilation angle ψ, and cohesion intercept *c'* for its failure criterion. In the following, the characteristics of Mohr-Coulomb model in ABAQUS are explained.

The Mohr-Coulomb failure criterion assumes that the failure occurs when the shear stress on any point in a soil mass reaches a value that depends linearly on the normal stress in the same plane. Mohr-Coulomb model is based on plotting Mohr's circle for states of stress at failure in the plane of the maximum and minimum principal stresses. The failure line is the best straight line that touches these Mohr's circles as shown in Fig. 3-3. Therefore, the Mohr-Coulomb failure criterion is defined by;

$$\tau = c' + \sigma' \times \tan \phi \qquad \text{....................} \quad (3\text{-}1)$$

where τ is the shear stress, *c'* is the cohesion intercept, σ' is the effective normal stress, and ϕ is the friction angle of soil.

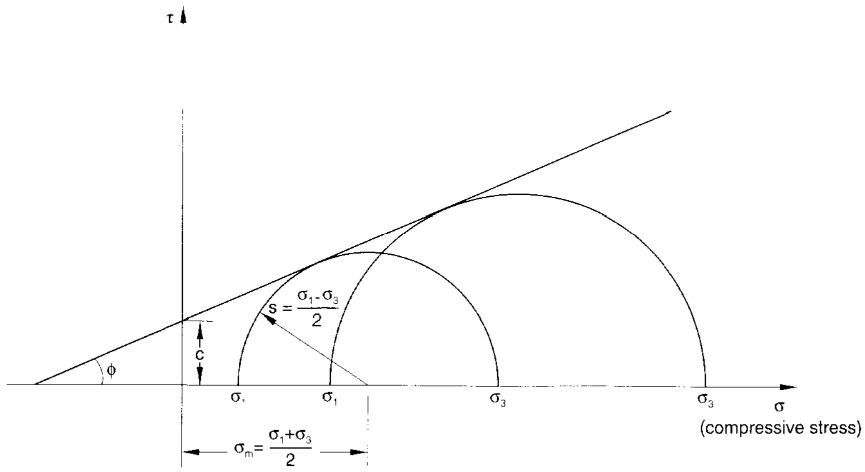

Figure 3-3 Mohr-Coulomb failure criterion in meridional plane

The friction angle ϕ controls the shape of the yield surface in the deviatoric plane as shown in Fig. 3-4. The friction angle can range from $0^\circ \leq \phi < 90^\circ$. In the case of $\phi = 0^\circ$, Mohr-Coulomb model reduces to the pressure-independent Tresca model with a perfectly hexagonal deviatoric section. In the case of $\phi = 90^\circ$, Mohr-Coulomb model reduces to the "tension cut-off" Rankine model with a triangular deviatoric section (this limiting case is not permitted within the Mohr-Coulomb model in ABAQUS).

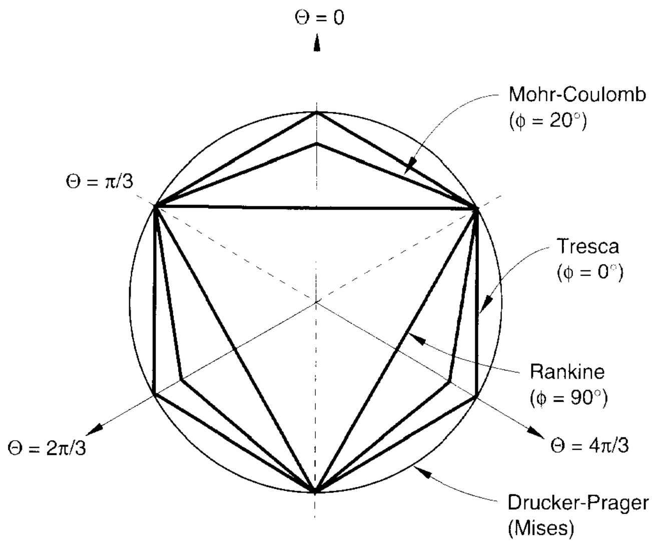

Figure 3-4 Mohr-Coulomb failure criterion in deviatoric plane
(Compressive stress is shown as negative in this figure.)

The flow potential is chosen as a hyperbolic function in the meridional stress plane as shown in Fig. 3-5 and as a smooth elliptic function proposed by Menetrey & William (1995) in the deviatoric plane as shown in Fig. 3-6.

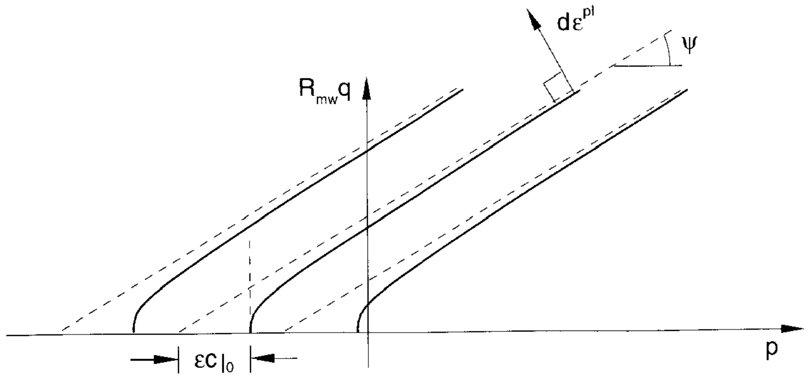

Figure 3-5 Mohr-Coulomb flow potential in meridional plane

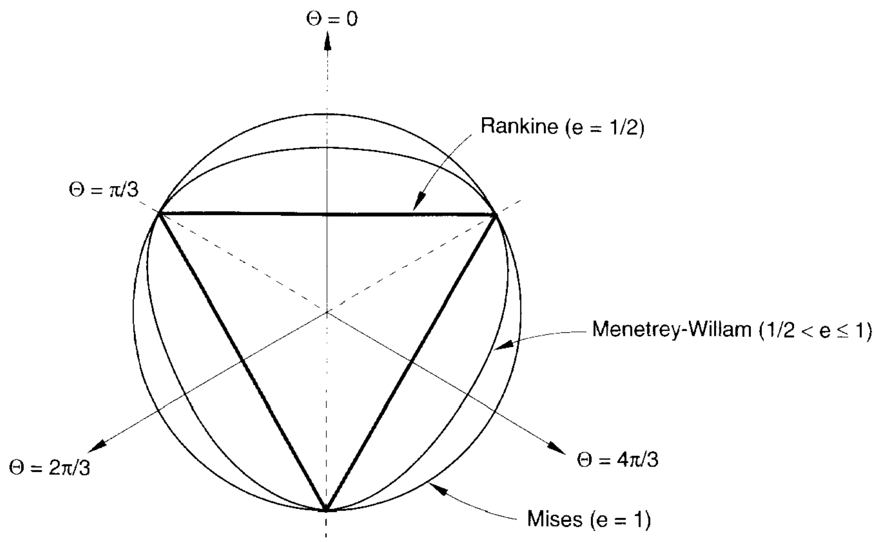

Figure 3-6 Mohr-Coulomb flow potential in deviatoric plane
(Compressive stress is shown as negative in this figure.)

By default, the deviatoric eccentricity e is automatically calculated by ABAQUS as defined in Eq. (3-2). This calculation corresponds to matching the flow potential to the yield surface in both triaxial compression and extension in the deviatoric plane.

$$e = \frac{3-\sin\phi}{3+\sin\phi} \qquad \text{.................... (3-2)}$$

Plastic flow in the meridional stress plane can be close to associated when the angle of friction ϕ and the angle of dilation ψ are equal and the meridional eccentricity ε is very small; however, plastic flow in this plane is generally non-associated. Plastic flow in the deviatoric stress plane is always non-associated. Therefore, the use of this Mohr-Coulomb model generally requires the unsymmetric matrix storage and solution scheme.

3.2.2 Clay plasticity soil model

The clay plasticity model provided in ABAQUS is an extension of Cam-Clay model (Schofield & Wroth, 1968). The model is based on the yield surface as;

$$\frac{1}{\beta^2}\left(\frac{p}{a}-1\right)^2 + \left(\frac{t}{Ma}\right)^2 - 1 = 0 \qquad \text{.................... (3-3)}$$

where $p = \frac{1}{3}\text{trace}\,\boldsymbol{\sigma}$ is the average confining pressure;

$t = \frac{1}{2}q\left[1+\frac{1}{K}-(1-\frac{1}{K})\left(\frac{r}{q}\right)^3\right]$ is the deviatoric stress;

$q = \sqrt{\frac{3}{2}\mathbf{S}:\mathbf{S}}$ is the Mises equivalent stress;

$r = \left(\frac{9}{2}\mathbf{S}:\mathbf{S}\cdot\mathbf{S}\right)^{\frac{1}{3}}$ is the third stress invariant;

M is a constant that defines the slope of the critical state line;

β is a constant that is equal to 1.0 on the "dry" side of the critical state line ($t > Mp$) but may be different from 1.0 on the "wet" side of the critical state line ($\beta \neq 1.0$ introduces a different ellipse on the wet side of the critical state line; i.e. a tighter "cap" is obtained if $\beta < 1.0$ as shown in Fig. 3-7.

a_o is a hardening parameter that defines the size of the yield surface; and

K is the ratio of the flow stress in triaxial extension to the flow stress in triaxial compression and determines the shape of the yield surface in the plane of principal deviatoric stresses (the Π-plane) (see Fig. 3-8).

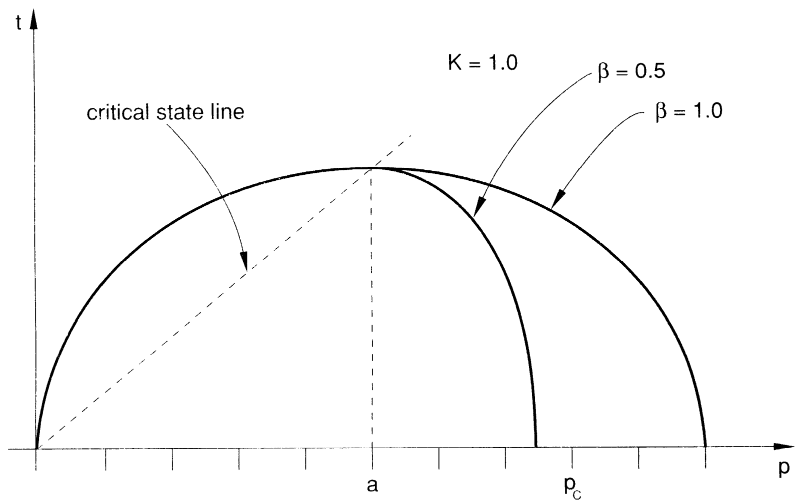

Figure 3-7 Clay yield surface in *p-t* plane

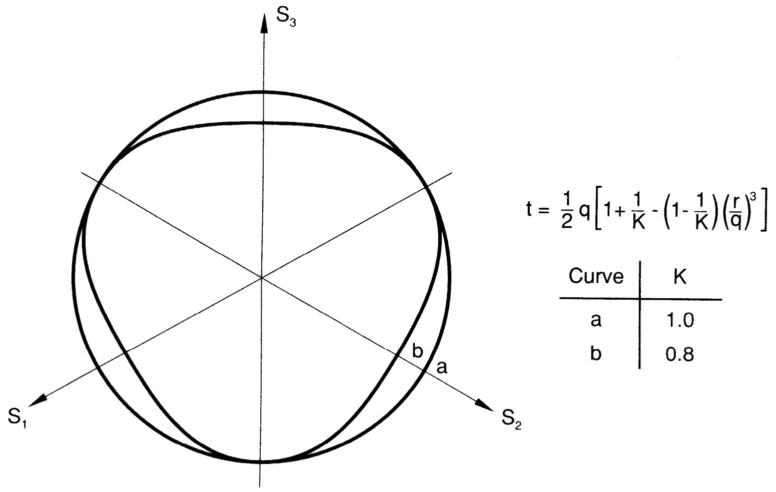

Figure 3-8 Clay yield surface section in Π-plane

(Compressive stress is shown as negative in this figure.)

The hardening law defining the size of the yield surface at any time is determined by the initial value of the hardening parameter a_o and the amount of plastic volumetric strain that occurs according to equation;

$$a = a_o \exp\left[\frac{1+\boldsymbol{e_o}}{\lambda-\kappa}\Delta\varepsilon_{vol}^{plastic}\right] \qquad \text{.................... (3-4)}$$

where $\Delta\varepsilon_{vol}^{plastic}$ is the plastic volumetric strain (compression is positive);

κ is the logarithmic bulk modulus of the material;

λ is the logarithmic hardening constant;

e_o is the initial void ratio.

a_o can be defined by specifying e_1, which is the intercept of the virgin consolidation line with the void ratio axis in the plot of void ratio e versus the logarithm of the effective confining pressure ln p (see Fig. 3-9). a_o is defined as;

$$a_o = \frac{1}{2}\exp\left(\frac{e_1 - e_o - \kappa \ln p_o}{\lambda-\kappa}\right) \qquad \text{.................... (3-5)}$$

where p_o is the initial value of the equivalent hydrostatic pressure stress.

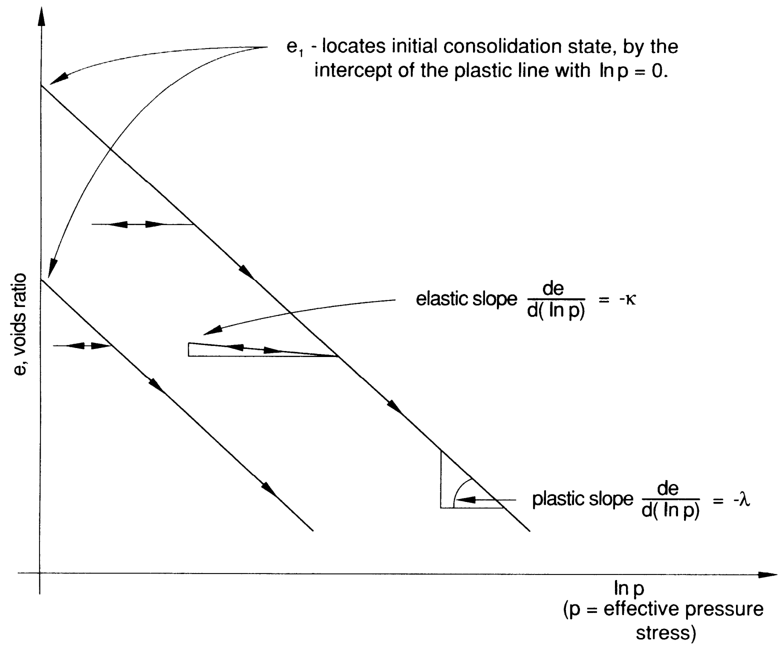

Figure 3-9 Pure compression behaviour for clay model

3.3 Input parameters

3.3.1 Pipe

(according to ASTM F 679-86: type T-2)

Material:	Poly Vinyl Chloride (PVC)
Nominal pipe diameter:	36 in.
Average outside diameter:	1000 mm
Average inside diameter:	942.6 mm
Wall thickness:	28.7 mm
Modulus of elasticity in tension:	2758 MPa
Poisson's ratio:	0.3
Density:	14.0 kN/m^3

3.3.2 Sand backfill

(assumed properties of dense sand from Trautmann & O'Rourke (1983) and Yimsiri et al. (2004))

Young's modulus *E*:	2894 kPa
Poisson's ratio ν:	0.3
Peak friction angle ϕ_{peak}:	44°

Dilation angle ψ:	16°
Initial void ratio e_o:	0.584
Initial dry density γ_{dry}:	17.7 kN/m3
Initial saturated density γ_{sat}:	21.4 kN/m3
Initial submerged density γ':	11.4 kN/m3

3.3.3 Clay

(assumed properties of Bangkok Clay from Balasubramaniam & Chaudhry (1978), Kuwano & Bhattarai (1989), and Tamrakar et al. (2000))

Slope of critical state line in triaxial compression M_{TC}:	1.0 ($\phi_{crit\ TC}$ = 25.4°)
Slope of critical state line in triaxial extension M_{TE}:	0.8
Ration of M_{TE}:M_{TC} (K):	0.8
Slope of normal compression line λ:	0.50
Slope of reloading line κ:	0.05
Void ratio of ICL at p' = 1 kPa:	4.012
Poisson's ratio ν:	0.3
Constant defining shape of yield surface in p-t plane β:	1.0
Coefficient of earth pressure at rest K_o:	0.6
Initial void ratio e_o:	2.0
Undrained shear strength s_u:	15 kPa
Saturated unit weight γ_{sat}:	17.0 kN/m^3
Dry unit weight γ_{dry}:	10.3 kN/m^3
Submerged unit weight γ':	7.2 kN/m^3
Coefficient of permeability k:	5×10^{-11} m/s

3.3.4 Interface between pipe and sand

Interface friction angle ϕ_μ (pipe-sand) = 22° (=ϕ_{peak}/2) (always modelled)

3.3.5 Interface between sand and clay

Interface friction angle ϕ_μ (sand-clay) = 25.4° (=ϕ_{crit}) (if modelled)

3.4 Finite element analysis procedures

The FE procedures can be categorised into two types, i.e. with and without construction sequences modelling. For the case of without construction sequences modelling, the sand (bedding, haunching, and backfill) and pipe are placed into the trench simultaneously within a very short time. For the case of with construction sequences modelling, the backfilling of the trench is done in step-by-step by placing bedding and pipe, haunching, and backfill, in step. In the following, the modelling procedures of these two types are explained.

3.4.1 Without construction sequences modelling

Step 1: Geostatic (1 sec)

Body force due to gravity: all elements = 7.19 kN/m^3

Excess pore water pressure boundary condition Δu = 0: top surface

Step 2: Trench excavation (1 sec)

Remove trench elements

Body force due to gravity: clay elements = 7.19 kN/m^3

Excess pore water pressure boundary condition Δu = 0: top surface

Step 3: Place bedding, pipe, haunching, backfill in dry condition (1 sec)

Add bedding, pipe, haunching, and backfill elements, strain free

Body force due to gravity: clay elements = 7.19 kN/m^3
sand elements = 17.7 kN/m^3
pipe elements = 14.0 kN/m^3

Excess pore water pressure boundary condition Δu = 0: top surface

Step 4: Trench flooding (fill trench with water) (1 sec)

Body force due to gravity: clay elements = 7.19 kN/m^3
sand elements = 11.4 kN/m^3
pipe elements = 4.0 kN/m^3

Excess pore water pressure boundary condition Δu = 0: top surface
trench boundary

Step 5: Long-term consolidation of clay (200 years)

Excess pore water pressure boundary condition Δu = 0: top surface
trench boundary

3.4.2 With construction sequences modelling

Step 1: Geostatic (1 sec)

Body force due to gravity: all elements = 7.19 kN/m^3

Excess pore water pressure boundary condition Δu = 0: top surface

Step 2: Trench excavation (1 sec)

Remove trench elements

Body force due to gravity: clay elements = 7.19 kN/m^3

Excess pore water pressure boundary condition Δu = 0: top surface

Step 3: Place bedding and pipe in dry condition (1 sec)

Add bedding and pipe elements, strain free

Body force due to gravity: clay elements = 7.19 kN/m^3
bedding elements = 17.7 kN/m^3
pipe elements = 14.0 kN/m^3

Excess pore water pressure boundary condition Δu = 0: top surface

Step 4: Place haunching in dry condition (1 sec)

Add haunching, strain free

Body force due to gravity: clay elements = 7.19 kN/m^3
bedding and hauncing elements = 17.7 kN/m^3
pipe elements = 14.0 kN/m^3

Excess pore water pressure boundary condition Δu = 0: top surface

Step 5: Place backfill in dry condition (1 sec)

Add backfill elements, strain free

Body force due to gravity: clay elements = 7.19 kN/m^3
sand elements = 17.7 kN/m^3
pipe elements = 14.0 kN/m^3

Excess pore water pressure boundary condition Δu = 0: top surface

Step 6: Trench flooding (fill trench with water) (1 sec)

Body force due to gravity: clay elements = 7.19 kN/m^3
sand elements = 11.4 kN/m^3
pipe elements = 4.0 kN/m^3

Excess pore water pressure boundary condition Δu = 0: top surface
trench boundary

Step 7: Long-term consolidation of clay (200 years)

Excess pore water pressure boundary condition Δu = 0: top surface

trench boundary

3.4.3 Dummy elements

When the trench elements are removed to simulate the trench excavation, the outside nodes (the nodes on the sand/clay interface) displace with the mesh, whereas the inside nodes remain at their current location because they are inactive. This may lead to convergence problems in cases where elements are severely distorted upon reactivation. This problem can be eliminated if the inner nodes are allowed to follow the outer nodes prior to reactivation. One option is done by overlaying the elastic elements of very low stiffness on the sand elements. These "dummy" elements use the same nodes as the sand elements but are so compliant that their effect on the analysis is negligible. They remain active throughout the analysis and ensure that the inner nodes follow the outer nodes.

This "dummy elements" strategy is employed in the present finite element analysis. The use of dummy elements alleviates the convergence problems when sand elements are reactivated to simulate backfilling.

3.5 Finite element analysis program

A total of 16 FE analyses were performed in this study. Their details are shown in Table 3-1.

Table 3-1 Finite element analysis program

Analysis name	With/without construction sequence	With/without interface between sand and clay	Trench depth (m)	Trench width (m)
D20W15(nocon)	Without	Without	2.0	1.5
D20W15int(nocon)	Without	With	2.0	1.5
D20W20(nocon)	Without	Without	2.0	2.0
D20W20int(nocon)	Without	With	2.0	2.0
D30W15(nocon)	Without	Without	3.0	1.5
D30W15int(nocon)	Without	With	3.0	1.5
D30w20(nocon)	Without	Without	3.0	2.0
D30W20int(nocon)	Without	With	3.0	2.0
D20W15(withcon)	With	Without	2.0	1.5
D20W15int(withcon)	With	With	2.0	1.5
D20W20(withcon)	With	Without	2.0	2.0
D20W20int(withcon)	With	With	2.0	2.0
D30W15(withcon)	With	Without	3.0	1.5
D30W15int(withcon)	With	With	3.0	1.5
D30w20(withcon)	With	Without	3.0	2.0
D30W20int(withcon)	With	With	3.0	2.0

Chapter 4 Finite element analysis results

The FE analysis results in term of vertical displacement of trench base and pipe base are summarised in Tables 4-1 and 4-2. The normal stresses exerted on the pipe after trench backfilling are summarized in Table 4-3. In the following, the results with respect to the parameters of interest are discussed.

Table 4-1 FE analysis results of no construction sequences modelling

Analysis name	Vertical movement of trench base (mm)				Vertical movement of pipe base (mm)		
	Excavation	Backfill	Trench flooding	Long-term consoln	Backfill	Trench flooding	Long-term consoln
D20W15 (nocon)	0 ↓ 14.45	14.45 ↓ 14.35	14.35 ↓ 10.53	10.53 ↓ 1.52	0 ↓ -0.21	-0.21 ↓ -4.24	-4.24 ↓ -13.44
D20W15int (nocon)	0 ↓ 14.46	14.46 ↓ 13.91	13.91 ↓ 4.84	4.84 ↓ -0.53	0 ↓ -0.69	-0.69 ↓ -9.83	-9.83 ↓ -15.27
D20W20 (nocon)	0 ↓ 16.12	16.12 ↓ 14.92	14.92 ↓ 3.29	3.29 ↓ -1.03	0 ↓ -1.52	-1.52 ↓ -13.27	-13.27 ↓ -17.65
D20W20int (nocon)	0 ↓ 16.15	16.15 ↓ -3.55	-3.55 ↓ -0.78	-0.78 ↓ -3.03	0 ↓ -20.10	-20.10 ↓ -17.19	-17.19 ↓ -19.45
D30W15 (nocon)	0 ↓ 15.99	15.99 ↓ -1.38	-1.38 ↓ 2.41	2.41 ↓ -0.17	0 ↓ -18.00	-18.00 ↓ -14.05	-14.05 ↓ -16.68
D30W15int (nocon)	0 ↓ 16.01	16.01 ↓ 0.32	0.32 ↓ 0.83	0.83 ↓ -2.31	0 ↓ -16.00	-16.00 ↓ -15.41	-15.41 ↓ -18.58
D30W20 (nocon)	0 ↓	18.08 ↓	14.53 ↓	2.87 ↓	0 ↓	-3.93 ↓	-15.69 ↓

	18.08	14.53	2.87	-1.61	-3.93	-15.69	-20.24
D30W20int (nocon)	0 ↓ 18.15	18.15 ↓ 18.15	18.15 ↓ 18.13	18.13 ↓ 6.85	0 ↓ -0.02	-0.02 ↓ -0.13	-0.13 ↓ -11.53

Table 4-2 FE analysis results of with construction sequences modelling

Analysis name	**Vertical movement of trench base (mm)**				**Vertical movement of pipe base (mm)**		
	Excavation	**Backfill**	**Trench flooding**	**Long-term consoln**	**Backfill**	**Trench flooding**	**Long-term consoln**
D20W15 (withcon)	0 ↓ 14.45	14.45 ↓ -3.43	-3.43 ↓ 1.29	1.29 ↓ 1.29	0 ↓ -18.63	-18.63 ↓ -13.72	-13.72 ↓ -13.72
D20W15int (withcon)	0 ↓ 14.46	14.46 ↓ 6.90	6.90 ↓ 2.85	2.85 ↓ -1.35	0 ↓ -8.10	-8.10 ↓ -12.05	-12.05 ↓ -16.26
D20W20 (withcon)	0 ↓ 16.12	16.12 ↓ -5.61	-5.61 ↓ 0.23	0.23 ↓ 0.23	0 ↓ -22.57	-22.57 ↓ -16.50	-16.50 ↓ -16.50
D20W20int (withcon)	0 ↓ 16.15	16.15 ↓ -2.04	-2.04 ↓ -0.54	-0.54 ↓ -2.20	0 ↓ -18.79	-18.79 ↓ -17.17	-17.17 ↓ -18.82
D30W15 (withcon)	0 ↓ 15.99	15.99 ↓ -2.45	-2.45 ↓ 1.62	1.62 ↓ 1.66	0 ↓ -18.97	-18.97 ↓ -14.74	-14.74 ↓ -14.73
D30W15int (withcon)	0 ↓ 16.01	16.01 ↓ 5.53	5.53 ↓ 0.51	0.51 ↓ -2.75	0 ↓ -10.69	-10.69 ↓ -15.63	-15.63 ↓ -18.86
D30W20 (withcon)	0 ↓ 18.08	18.08 ↓ -4.79	-4.79 ↓ 0.19	0.19 ↓ 0.22	0 ↓ -23.62	-23.62 ↓ -18.44	-18.44 ↓ -18.43

D30W20int (withcon)	0 ↓ 18.15	18.15 ↓ -9.43	-9.43 ↓ -2.53	-2.53 ↓ -5.04	0 ↓ -28.03	-28.03 ↓ -20.95	-20.95 ↓ -23.47

Table 4-3 Normal stress exerted on pipe after trench backfilling

Analysis name	Normal stress exerted on pipe	
	During trench flooding	During long-term consoln
D20W15(nocon)	Increase	Increase
D20W15int(nocon)	Increase	Slightly increase
D20W20(nocon)	Increase	Slightly increase
D20W20int(nocon)	Decrease	Same
D30W15(nocon)	Decrease	Same
D30W15int(nocon)	Slightly decrease	Same
D30W20(nocon)	Increase	Same
D30W20int(nocon)	Increase	Same
D20W15(withcon)	Decrease	Same
D20W15int(withcon)	Increase	Slightly increase
D20W20(withcon)	Decrease	Same
D20W20int(withcon)	Decrease	Same
D30W15(withcon)	Decrease	Same
D30W15int(withcon)	Increase	Same
D30W20(withcon)	Decrease	Same
D30W20int(withcon)	Decrease	Same

4.1 Effects of trench width and depth

The effects of trench width and depth on the pipeline-soil interaction are investigated by considering the results from the case of with interface modelling between sand/clay and with construction sequences modelling. These results are considered to be most realistic and closest to the real field situation. The vertical movements of the trench base and pipe base for the case of 3 m depth trench are shown in Fig. 4-1. The results for the case of 2 m depth trench also show similar pattern. Fig. 4-1 shows that the width of the trench affects responses of the trench and the pipe during construction process. After completion of backfilling, the trench base and pipe base settle less for narrow trench (1.5 m width) than for wide trench (2 m width). This is due to the near-field boundary effect of the side of the trench, which causes more arching effects for the case of narrow trench. As a result, less load transfers from sand backfill to trench base and pipe. This is substantiated by the results in Fig. 4-2 showing that, after the completion of sand backfilling, the vertical stress of sand exerted on the pipe is smaller for narrow trench than wide trench.

The behaviour after trench flooding is also different for narrow and wide trench. For narrow trench, the trench base and pipe base settle more after trench flooding, whereas heave is observed for wide trench (Fig. 4-1). For narrow trench, the normal stress exerted on the pipe increases after trench flooding, whereas it decreases for wide trench (Fig. 4-2). During long-term consolidation, the trench base and pipe base settle with time for both cases of trench width. For both cases, there is no difference in normal stress on the pipe during long-term consolidation. The effects of trench depth, for the range in this study (2 and 3 m), seem to be insignificant.

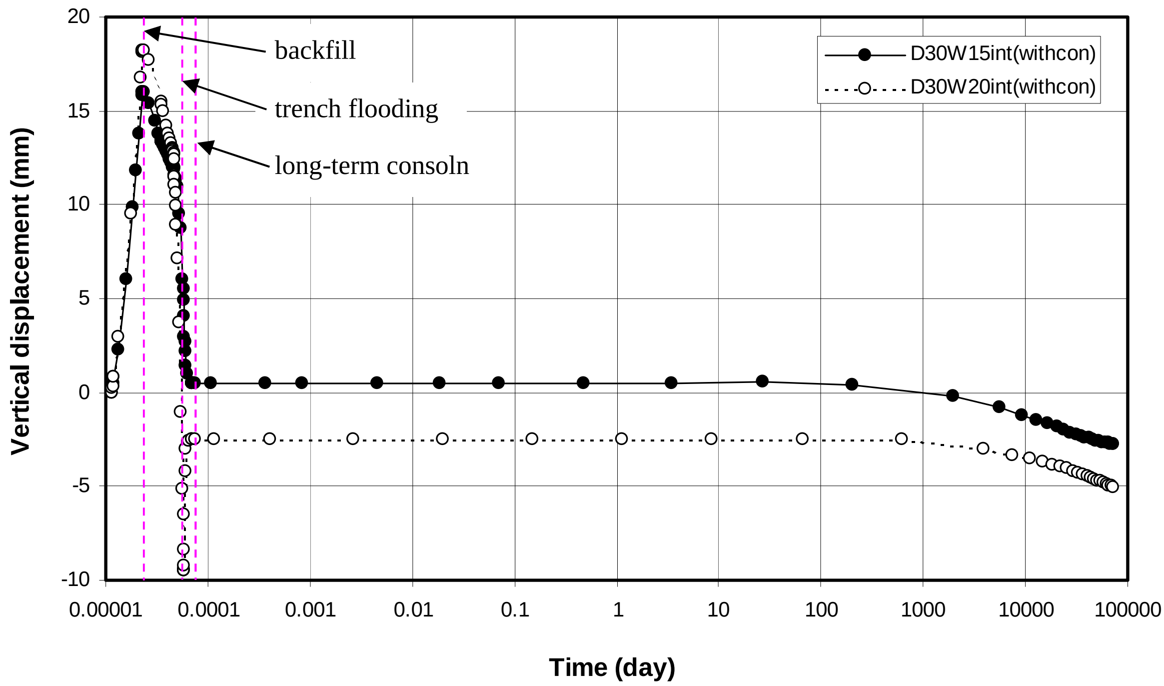

(a) Trench base

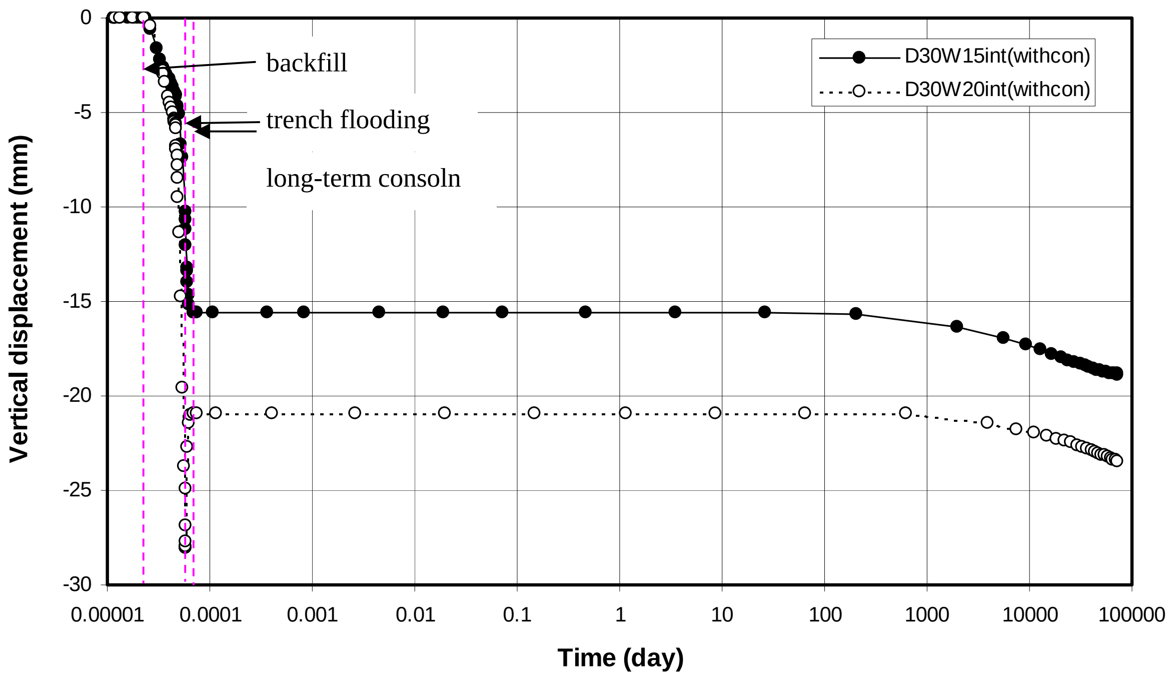

(b) Pipe base

Figure 4-1 Effects of trench width on vertical displacement of trench base and pipe base

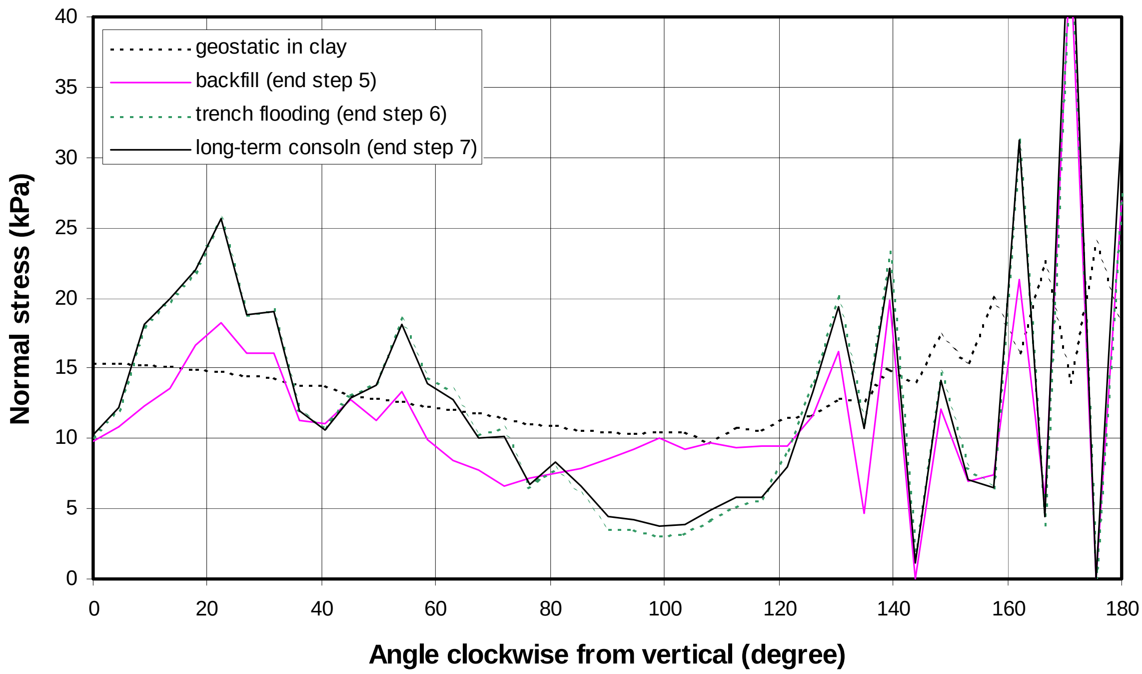

(a) Analysis: D30W15int(withcon)

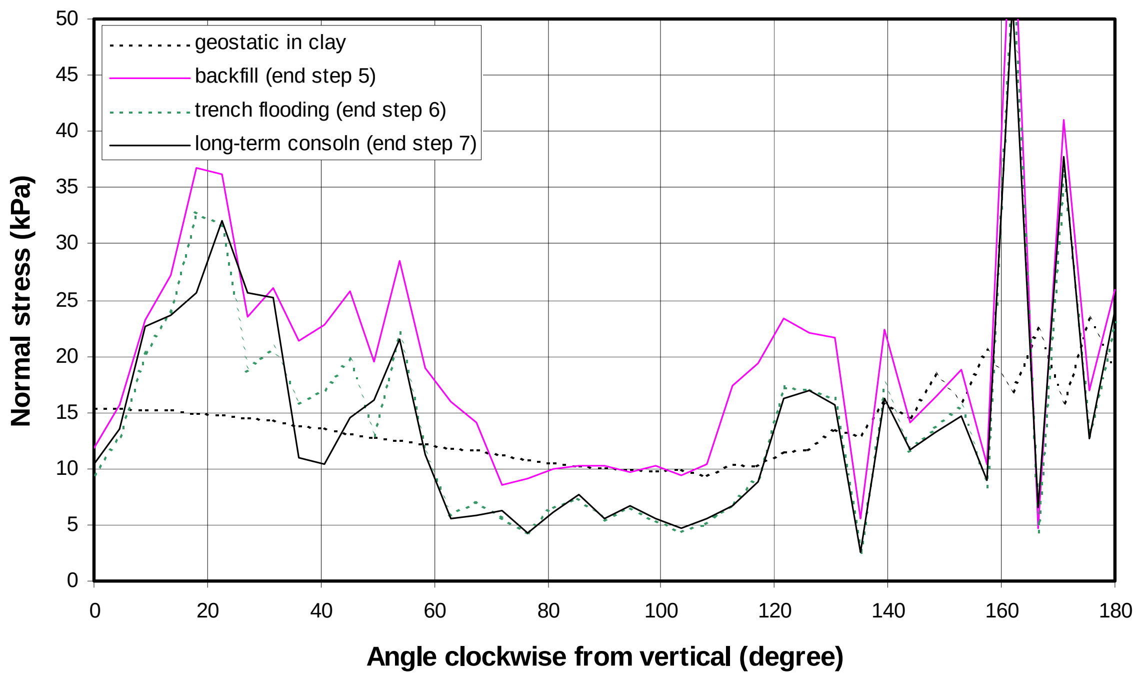

(b) Analysis: D30W20int(withcon)

Figure 4-2 Effects of trench width on normal stress exerted on pipe

4.2 Effects of interface between sand and clay

The importance of modelling the interface between sand backfill and clay trench is investigated by comparing the finite element analysis results between the cases with and without interface modelling. It was found that, immediately after backfilling, the cases of with interface modelling does not necessarily result in larger settlement compared to the cases of no interface modelling. Larger settlements are obtained for the cases of D20W15(nocon) vs D20W15int(nocon), D20W20(nocon) vs D20W20int(nocon), and D30W20(withcon) vs D30W20int(withcon) as shown in Fig. 4-3. For other cases, the results are opposite in which the settlements, after the completion of backfilling, of trench base and pipe base are larger for the cases of no interface modelling (Fig. 4-4). However, for all cases, the settlements of trench base and pipe base, at the end of trench flooding and long-term consolidation, are consistently larger for the cases of with interface modelling (except D30W20(nocon) vs D30W20int(nocon)). It is interesting to note that, for all cases of no interface modelling and with construction sequences modelling, there is almost no vertical displacement of trench base and pipe base during long-term consolidation.

For the cases of no construction sequences modelling, the normal stress exerted on the pipe, after completion of pipe installation and backfilling, is larger for the cases of with interface modelling (Fig. 4-5). However, the normal stresses are almost independent of interface modelling when the construction sequences are simulated (Fig. 4-6).

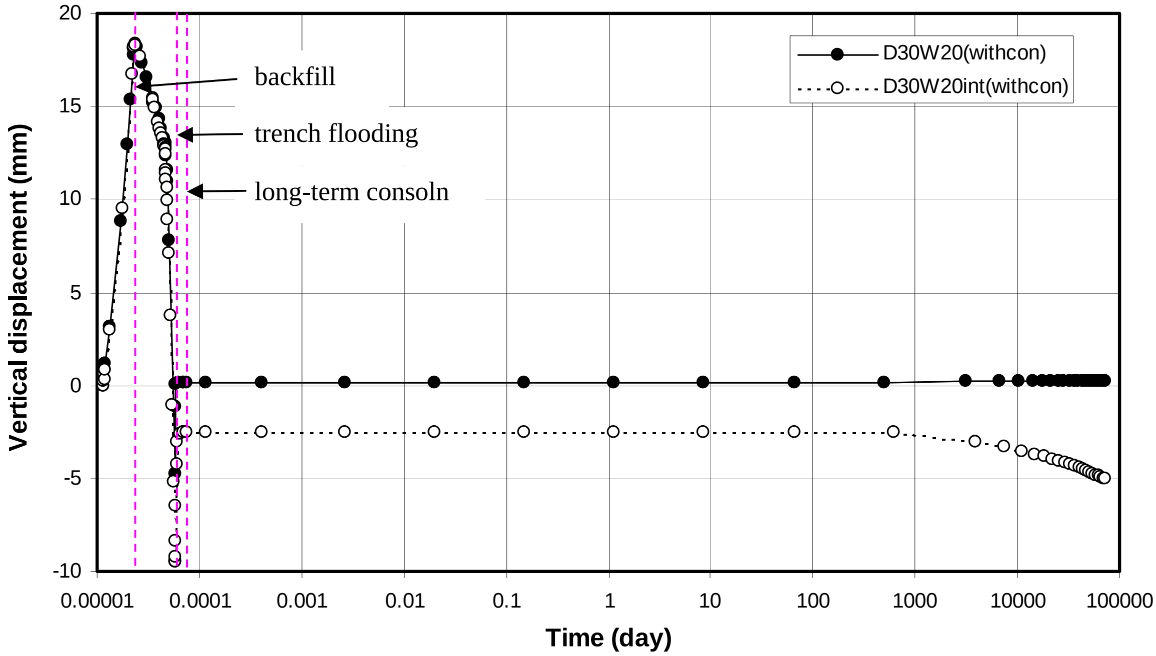

(a) Trench base

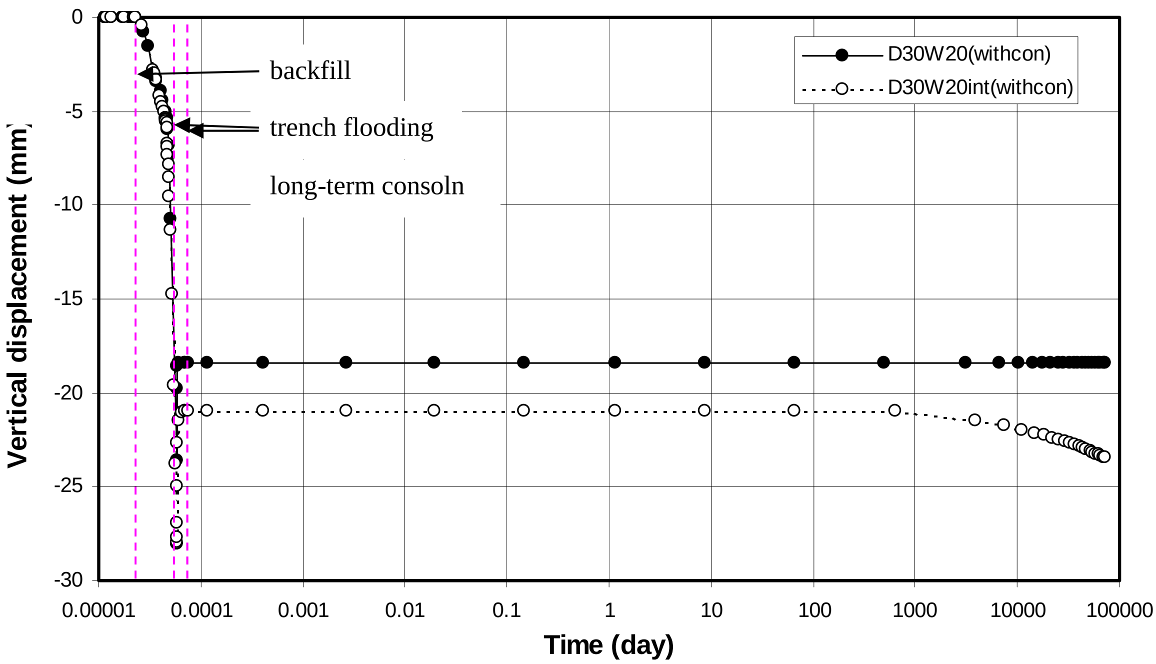

(b) Pipe base

Figure 4-3 Effects of modelling interface between sand/clay on vertical displacement of trench base and pipe base (with construction sequence modelling)

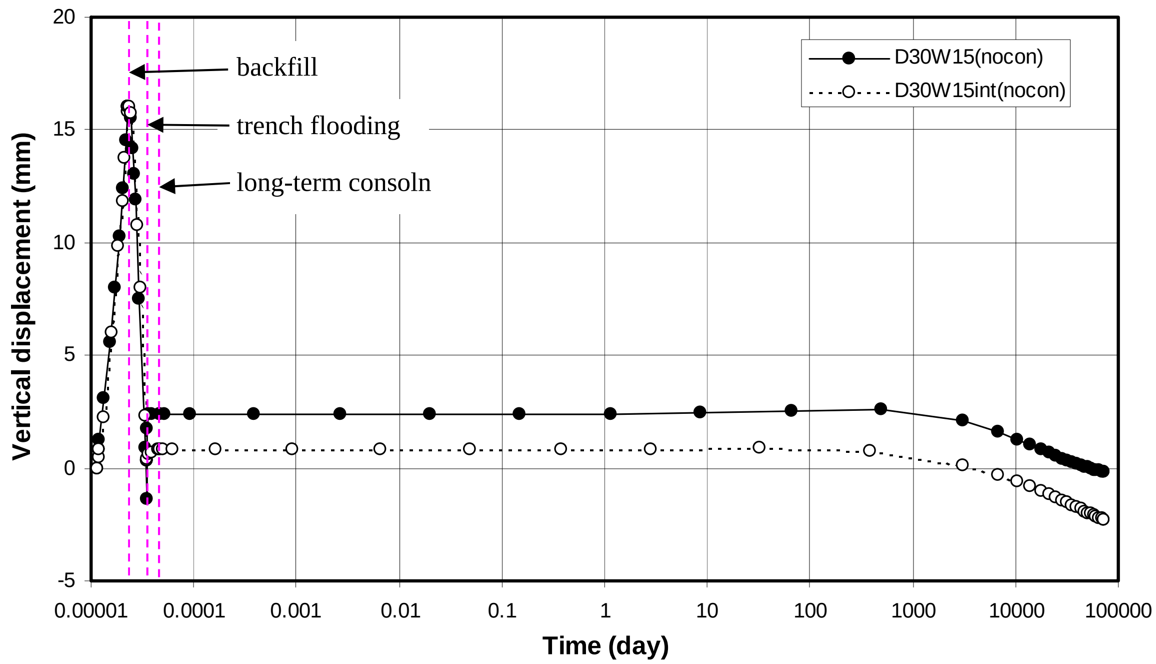

(a) Trench base

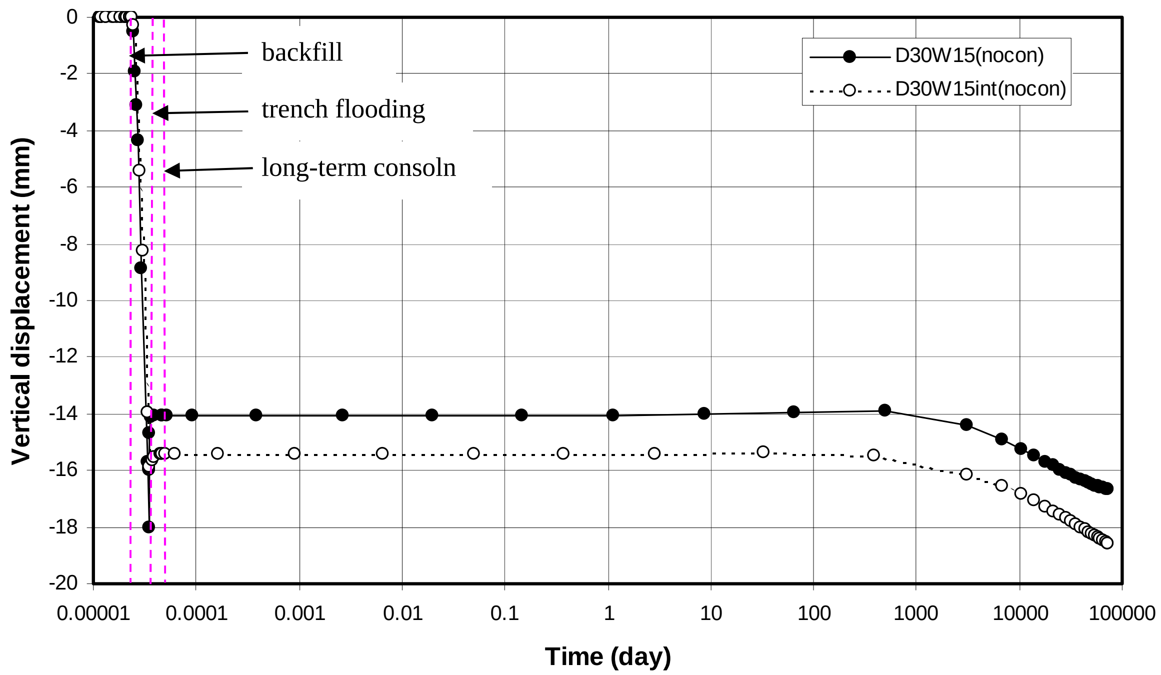

(b) Pipe base

Figure 4-4 Effects of modelling interface between sand/clay on vertical displacement of trench base and pipe base (without construction sequence modelling)

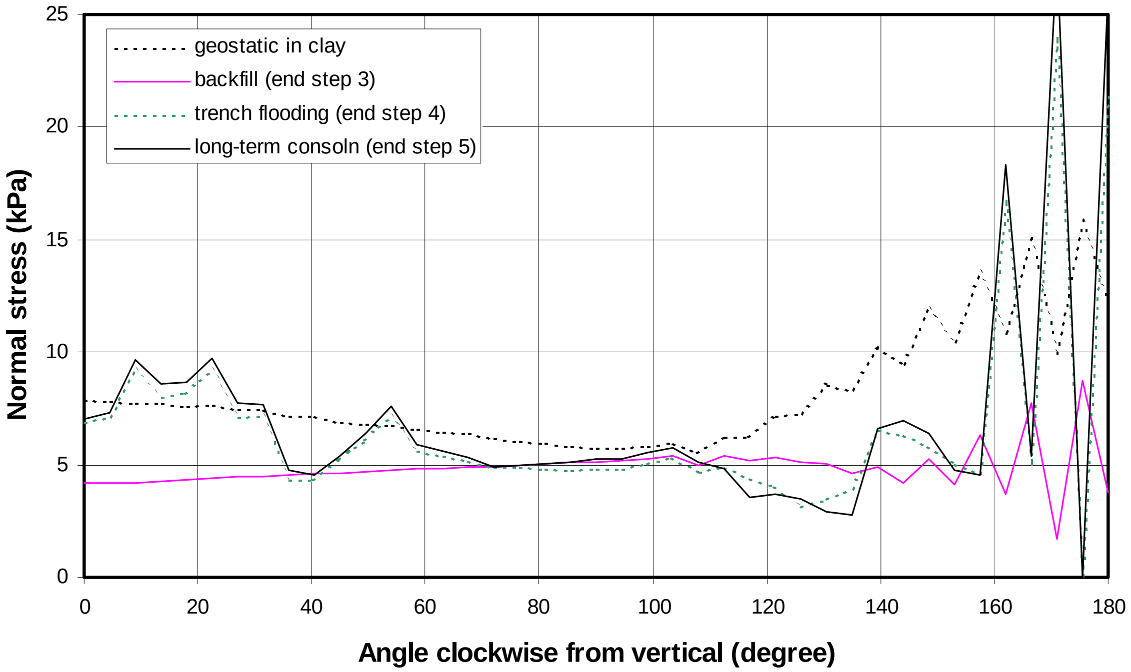

(a) Analysis: D20W20(nocon)

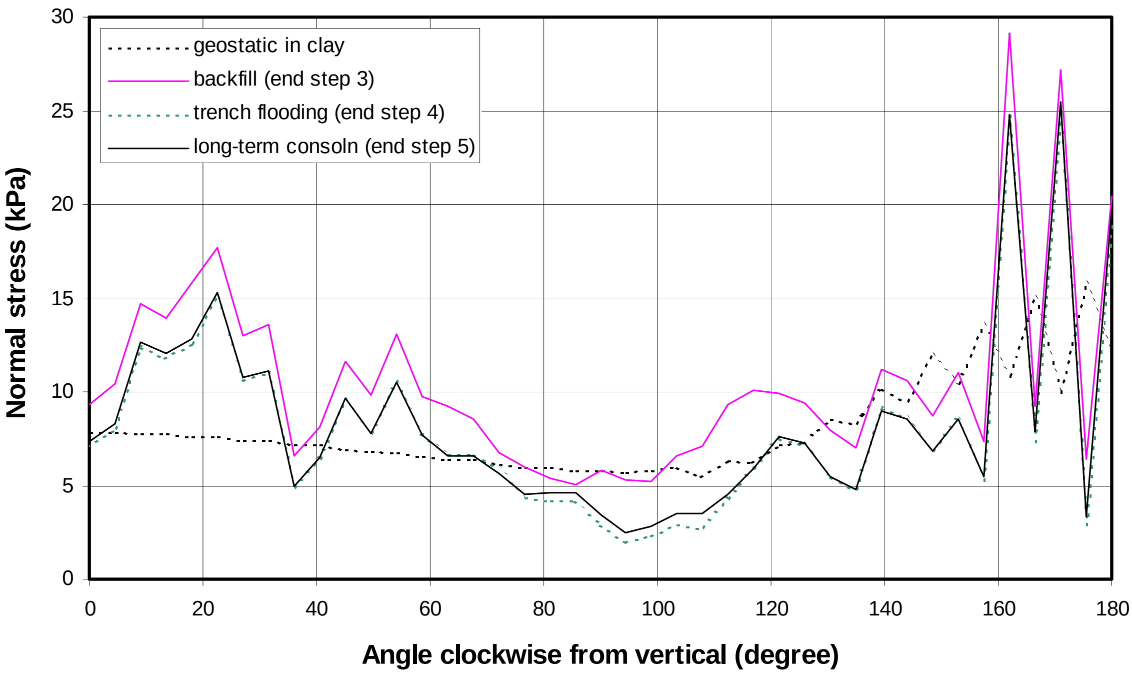

(b) Analysis: D20W20int(nocon)

Figure 4-5 Effects of modelling interface between sand/clay on normal stress exerted on pipe (without construction sequences modelling)

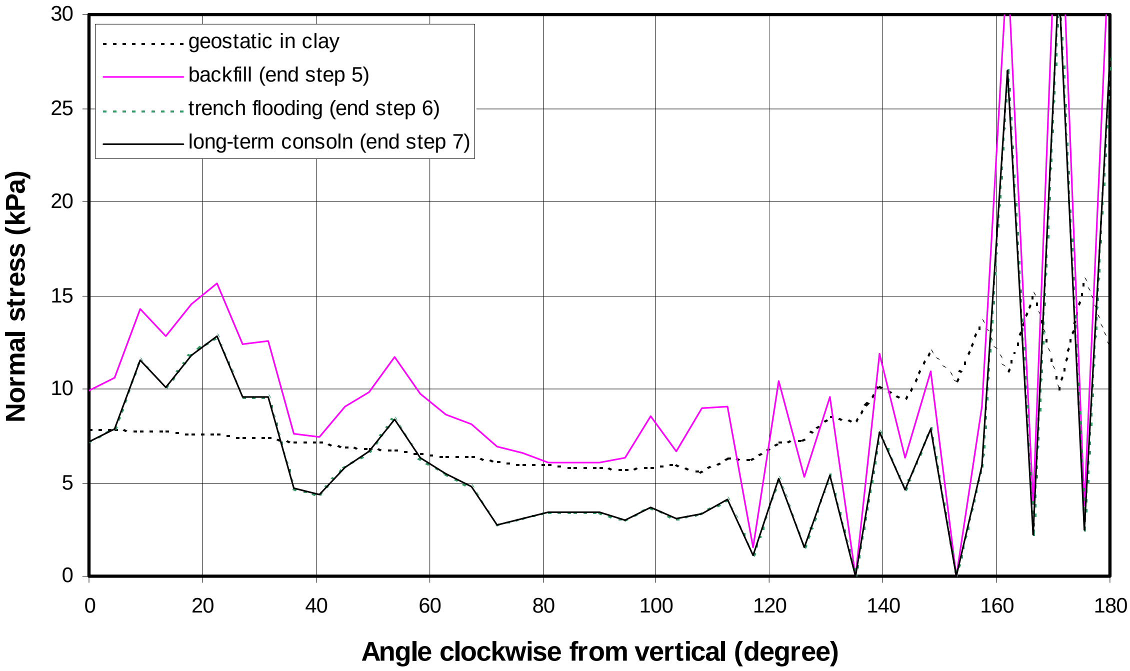

(a) Analysis: D20W20(withcon)

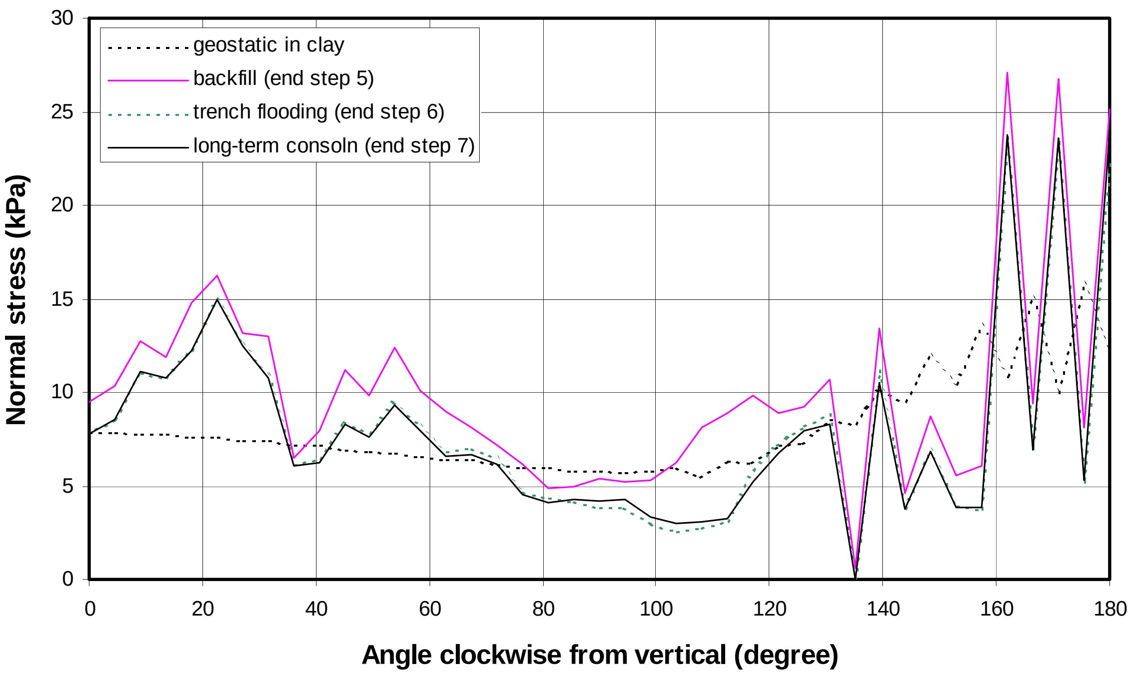

(b) Analysis: D20W20int(withcon)

Figure 4-6 Effects of modelling interface between sand/clay on normal stress exerted on pipe (with construction sequences modelling)

4.3 Effects of modelling construction sequences

The importance of modelling construction sequences is investigated by comparing the finite element analysis results between the cases of with and without construction sequences modelling. For the case of no interface modelling, the settlements of trench base and pipe base, after the completion of sand backfilling, are larger for the cases of with construction sequences modelling than for the cases of no construction sequences modelling (Fig. 4-7). However, when the interface is modelled, the vertical movements of trench base and pipe base for both with and without construction sequences modelling are comparable (Fig. 4-8) (except D30W15int(nocon) vs D30W15int(withcon) and D30W20int(nocon) vs D30W20int(withcon)). For all cases, the settlements at the end of long-term consolidation for the cases of no construction sequences modelling are slightly larger than those for the cases of with construction sequences modelling.

This larger settlement, after the completion of sand backfilling, for the case of with construction sequence modelling is possibly due to the larger normal stress exerted on the pipe by sand backfill. As can be seen in Fig. 4-9, the stress exerted on the pipe, after sand backfilling, for the case of with construction sequences modelling is larger than for the cases of no construction sequence modelling. When interface is modelled, the normal stresses are similar for both cases (Fig. 4-10).

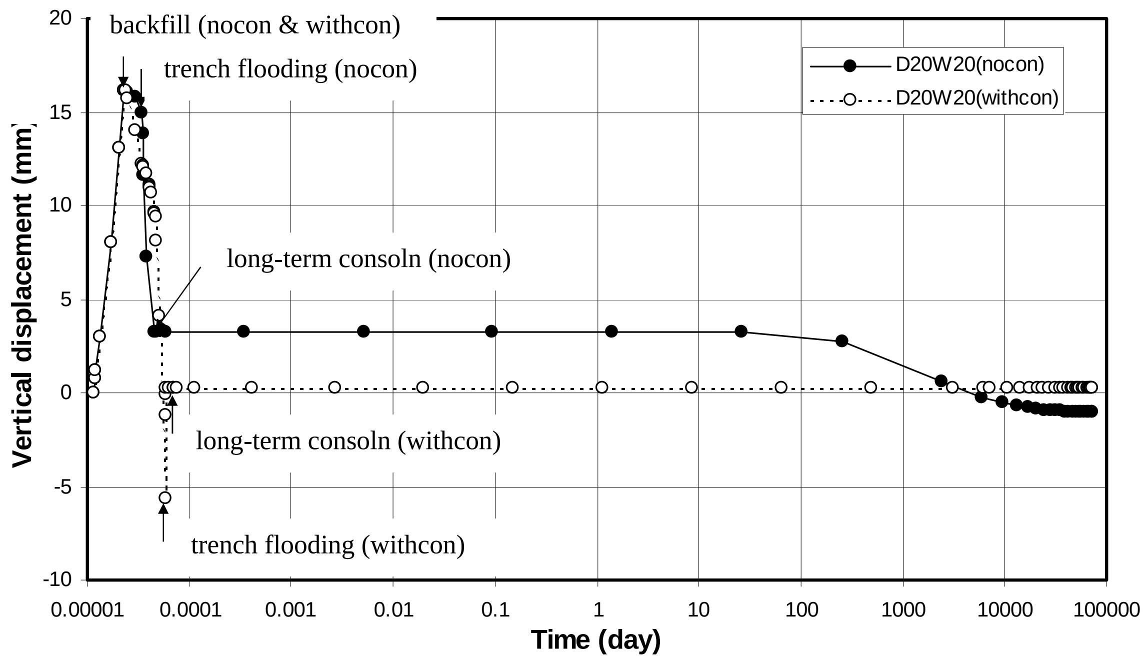

(a) Trench base

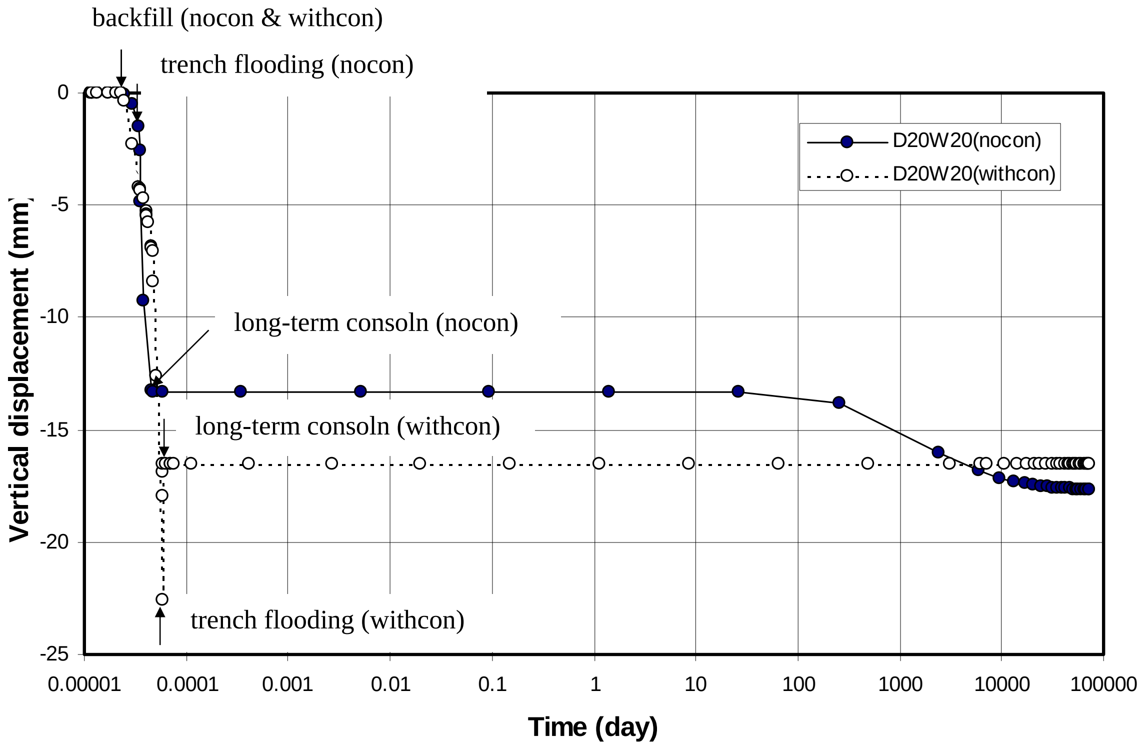

(b) Pipe base

Figure 4-7 Effects of construction sequences modelling for cases without modelling of interface between sand/clay

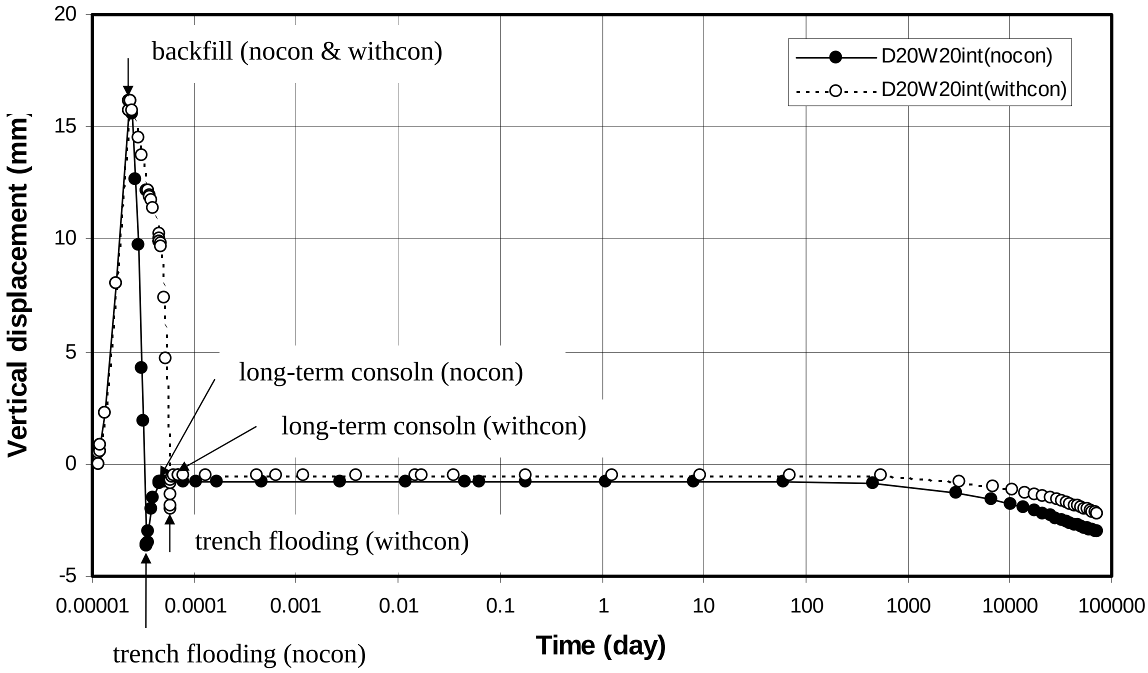

(a) Trench base

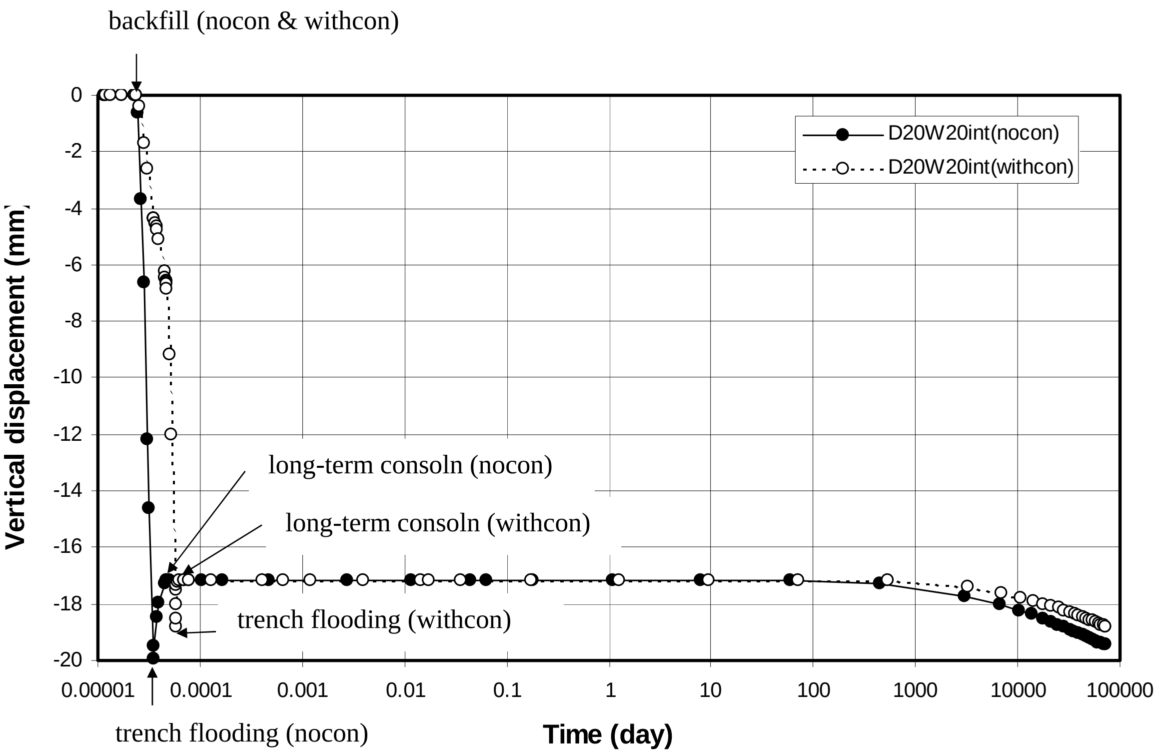

(b) Pipe base

Figure 4-8 Effects of construction sequences modelling for cases with modelling of interface between sand/clay

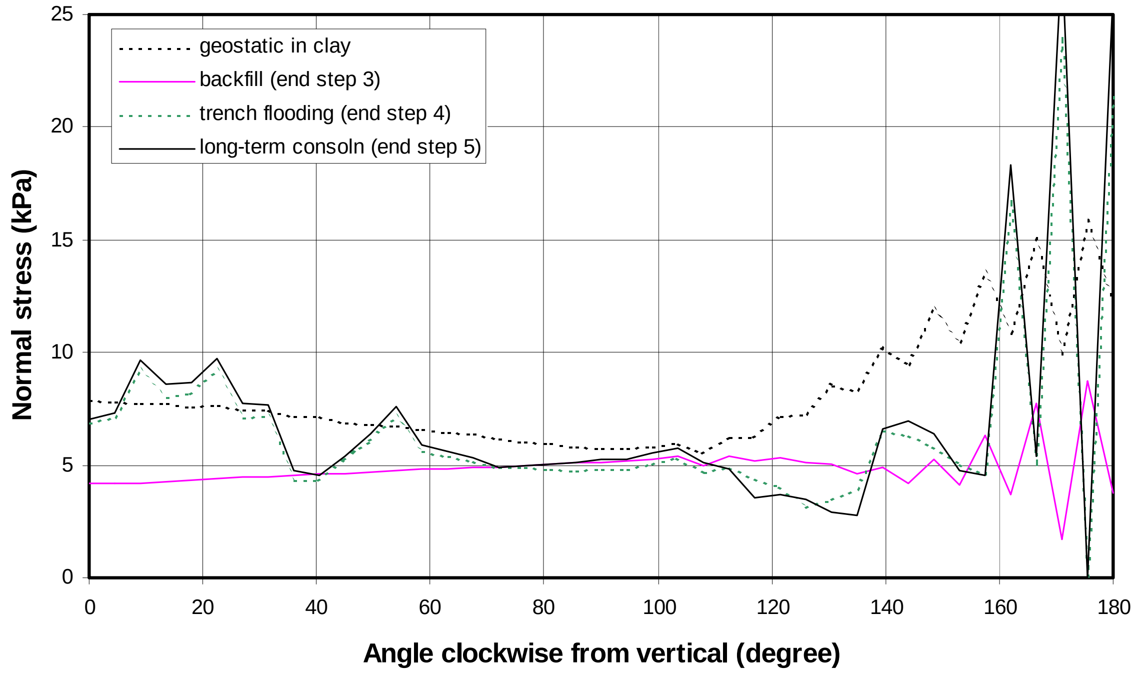

(a) Analysis: D20W20(nocon)

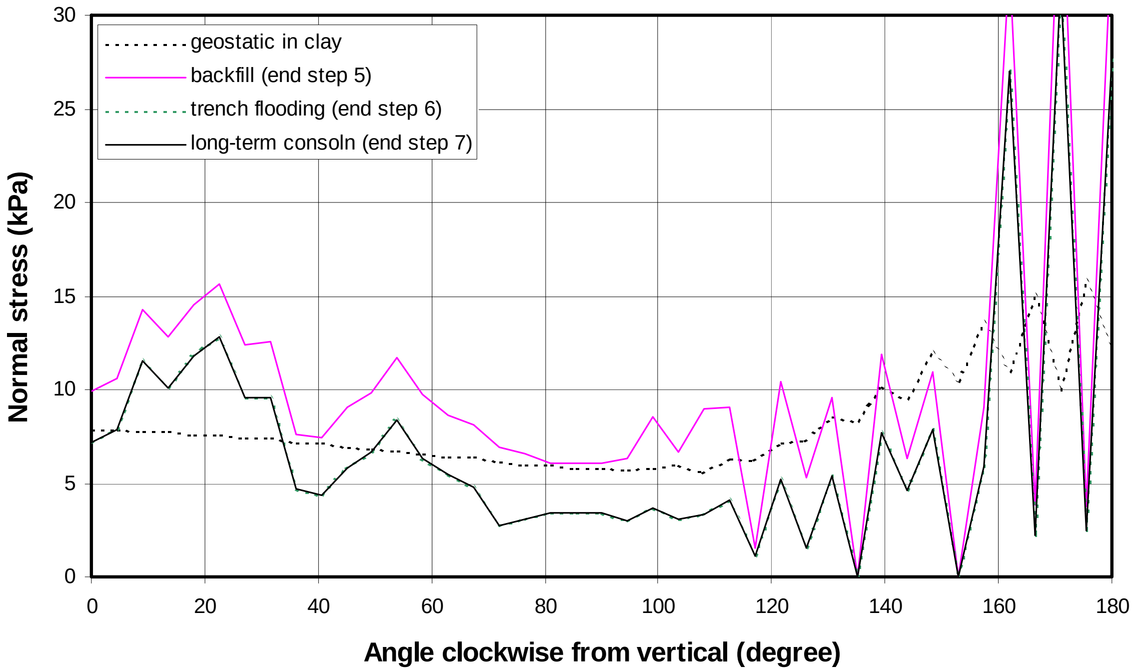

(b) Analysis: D20W20(withcon)

Figure 4-9 Effects of construction sequences modelling on normal stress exerted on pipe (without modelling of interface between sand/clay)

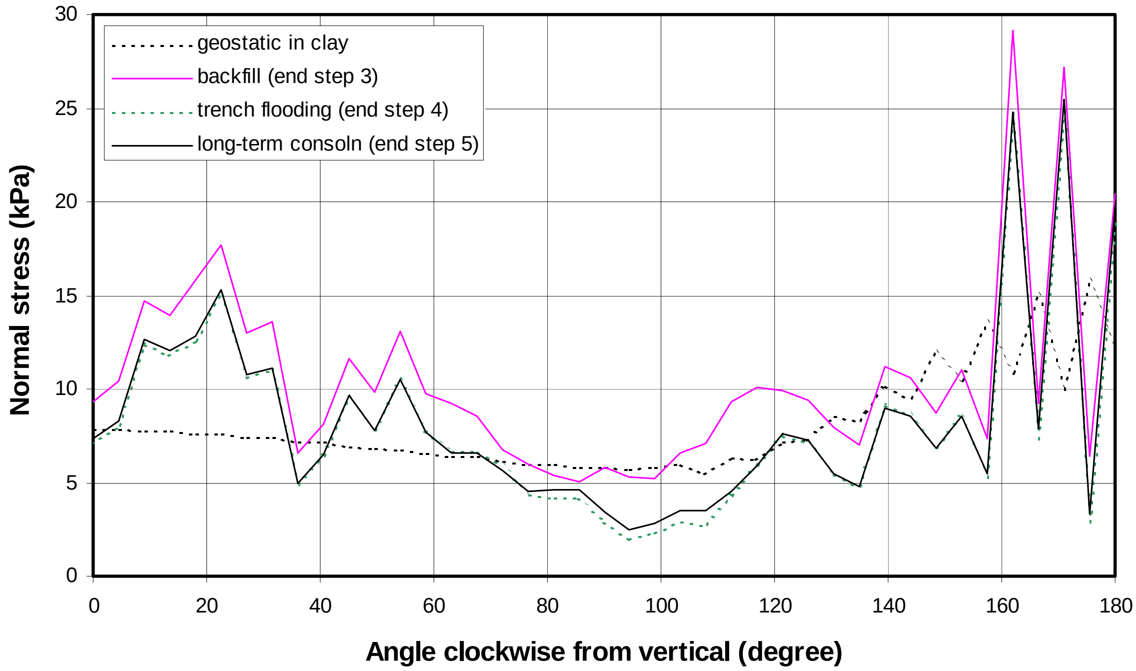

(a) Analysis: D20W20int(nocon)

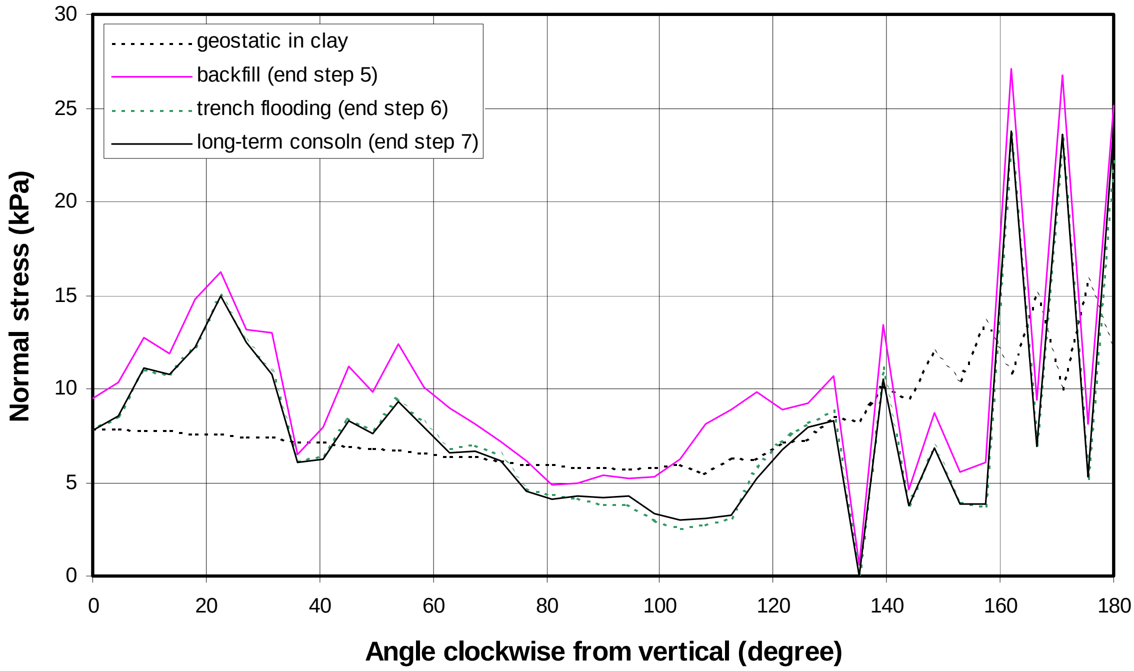

(b) Analysis: D20W20int(withcon)

Figure 4-10 Effects of construction sequences modelling on normal stress exerted on pipe (with modelling of interface between sand/clay)

Chapter 5 Conclusions

The finite element analysis is performed in this study to investigate the long-term pipeline-soil interaction of pipe buried in sand trench embedded in soft clay. The effects of trench dimensions, the importance of modelling interface between sand backfill and clay trench, and the importance of modelling construction sequence on the pipeline-soil interaction were investigated.

It was decided to decouple the long-term pipeline-soil response into two stages; (i) trench flooding and (ii) long-term consolidation. During trench flooding, the FE results show that the trench width has profound effects on the pipeline-soil response. For narrow trench (1.5-m width), the stress exerted on the pipe increases and the pipe settles more. This is due to the fact that narrow trench results in less normal stress from sand backfill exerted on the pipe after trench backfilling because of more arching effect above the pipe. During trench flooding, the pipe and sand backfill settle and adjust their interaction in a way that the sand backfill transfers more stress to the pipe and this, in turn, results in settlement again. For wide trench (2-m width), the stress exerted on the pipe decreases and the pipe moves up. This is due to the fact that wide trench has less arching effect after trench backfilling. During trench flooding, the predominant mechanism is a reduction in unit weight of the sand backfill and the pipe itself from dry unit weight to submerged unit weight. This results in less normal stress exerted on the pipe and heave. This is probably the most significant finding in this study.

During long-term consolidation, the pipe settles for both trench widths; however, there is practically no change in normal stress exerted on the pipe observed. After the changes in normal stresses during trench flooding for both cases (increasing for narrow trench and decreasing for wide trench), the normal stresses for both cases become equal during long-term consolidation.

In reality, the trench flooding and long-term consolidation occur at the same time for a long period. Hence, the combination of the behaviour during trench flooding and long-term consolidation can be considered as a long-term response in the field case. The FE results suggest that the long-term response of pipe depends strongly on trench widths but independent of trench depths (for the depths studied). Moreover, this long-term response is more likely to be due to the trench flooding (saturation) process, not consolidation of the surrounding clay.

Without interface and construction sequences modelling, the arching effect severely influences the FE analysis. The stress exerted on the pipe by sand backfill after trench backfilling is unrealistically small for this case. In order to obtain realistic results, both interface and construction sequences modelling should be employed in the FE analysis for pipeline-soil interaction problems in a trench.

เอกสารอ้างอิง

ASTM Designation: F 679-86, “Standard Specification for Poly(Vinyl Chloride) (PVC) Large-Diameter Plastic Gravity Sewer Pipe and Fittings”

ASTM Designation: F 690-86, “Standard Practice for Underground Installation of Thermoplastic Pressure Piping Irrigation Systems”

Balasubramaniam, A. S. and Chaudhry, A. R. (1978), “Deformation and Strength Characteristics of Soft Bangkok Clay”, *Journal of the Geotechnical Engineering Division*, ASCE, Vol. 104, No. GT9, pp. 1153-1167

Kuwano, J. and Bhattarai, B. N. (1989), “Deformation characteristics of Bangkok Clay under three dimensional stress conditions”, *Geotechnical Engineering*, SEAGS, Vol. 20, No. 2, pp. 111-137

Menetrey, Ph. and William, K. J. (1995), “Triaxial Failure Criterion for Concrete and its Generalization”, *ACI Structureal Journal*, Vol. 92, pp. 311-318

Schofield, A. N. and Wroth, C. P. (1968), *Critical State Soil Mechanics*, McGraw-Hill

Tamrakar, S. B., Shibuya, S., and Mitachi, T. (2000), “Parametric FE analysis on the behaviour of Bangkok Clay underneath test embankment at Nong Ngoo Hao”, *Geotechnical Engineering*, SEAGS, Vol. 31, No. 3, pp. 193-208

Trautmann, C. H. and O’Rourke, T. D. (1983), “Behavior of Pipe in Dry Sand Under Lateral and Uplift Loading”, *Geotechnical Engineering Report 83-7*, Cornell University

Yimsiri, S., Soga, K., Yoshizaki, K., Dasari, G. R., and O’Rourke, T. D. (2004), “Lateral and Upward Soil-Pipeline Interactions in Sand for Deep Embedment Conditions”, Journal of Geotechnical and Geoenvironmental Engineering, ASCE, Vol. 130, No. 8, pp. 830-842